Mushy magma beneath Yellowstone

Risheng Chu,[1] Don V. Helmberger,[1] Daoyuan Sun,[1] Jennifer M. Jackson,[1] and Lupei Zhu[2]

Received 3 November 2009; revised 2 December 2009; accepted 15 December 2009; published 15 January 2010.

[1] A recent prospective on the Yellowstone Caldera discounts its explosive potential based on inferences from tomographic studies which suggests a high degree of crystallization of the underlying magma body. In this study, we show that many of the first teleseismic *P*-wave arrivals observed at seismic stations on the edge of the caldera did not travel through the magma body but have taken longer but faster paths around the edge. After applying a number of waveform modeling tools, we obtain much lower seismic velocities than previous studies, 2.3 km/sec (V_p) and 1.1 km/sec (V_s). We estimate the physical state of the magma body by assuming a fluid-saturated porous material consisting of granite and a mixture of rhyolite melt and water and CO_2 at a temperature of 800°C and pressure at 5 km (0.1 GPa). We found that this relatively shallow magma body has a volume of over 4,300 km^3 and is about 32% melt saturated with about 8% water plus CO_2 by volume.
Citation: Chu, R., D. V. Helmberger, D. Sun, J. M. Jackson, and L. Zhu (2010), Mushy magma beneath Yellowstone, *Geophys. Res. Lett.*, *37*, L01306, doi:10.1029/2009GL041656.

1. Introduction

[2] The giant Yellowstone Caldera (supervolcano; Figure 1a), generated by an explosion about 640,000 years ago, has slumbered for over 70,000 years since the last eruption [*Christiansen*, 2001]. It is experiencing thousands of small earthquakes every year with $M_w \geq 6.0$ damaging events every few decades [*Waite and Smith*, 2002; *Husen et al.*, 2004]. It also has the world's largest hydrothermal system [*Fournier*, 1989; *Lowenstern et al.*, 2006] and emits 45,000 tons of CO_2 daily [*Werner and Brantley*, 2003]. Both GPS and InSAR observations suggest periodic uplift and subsidence of the caldera [*Wicks et al.*, 1998, 2006; *Puskas et al.*, 2007], and in mid-2004, the uplift accelerated to about 7 cm/year [*Chang et al.*, 2007] (Figure 1b). Apparently, the accelerated uplift is related to a magma recharge [*Chang et al.*, 2007]. Inversion of the GPS and InSAR data suggests a magma sill at shallow depths with an area of 1,200 km^2 and magma charge rate of about 0.1 km^3 yearly [*Chang et al.*, 2007], mapped out in Figure 1b. The shallow magma body beneath the Yellowstone Caldera is also the key to explaining the low Bouguer gravity anomaly [*Eaton et al.*, 1975] (Figure 1a). In order to reveal the size and velocity drop of the magma body, many seismological tomographic studies have been conducted using regional earthquake data [*Benz and Smith*, 1984; *Miller and Smith*, 1999; *Husen et al.*, 2004] and surface waves [*Stachnik et al.*, 2008]. A common feature among these results is that a low velocity zone (LVZ) lies beneath the caldera. Tomographic studies indicates that the *P*- and *S*-wave velocities drop by 10% [*Husen et al.*, 2004] and 20% [*Stachnik et al.*, 2008], respectively. Based on these velocities, a high degree of crystallization of the magma body was inferred [*Husen et al.*, 2004].

[3] Since the caldera is sitting above a complex upper mantle, it becomes difficult to isolate travel-time effects caused by the magma body using tomography. For this reason we concentrate on modeling the first few seconds of the *P*-waveform field as observed on broadband seismic systems. Although there were many short-period seismic surveys, only five broadband three component seismic stations are presently available as positioned in Figure 1, one US National Seismic Network station (LKWY), one USArray station (H17A) and three stations from the Yellowstone-Intermountain Seismic Array (YISA, Y100, Y102 and Y103). We obtained teleseismic waveforms from IRIS DMC with good signal-to-noise ratios from 359 earthquakes between January 1999 and November 2008 recorded by LKWY, 100 earthquakes between January 2008 and November 2008 recorded by station H17A, and 111 earthquakes between June 2000 and May 2001 recorded by YISA stations. All events have magnitude larger than 5.5 and distance range between 30° and 90° (See Figure S1).[3] Since most of the events are arriving from the NW and SE, we will address 2D cross-sections through the caldera indicated by the black lines in Figure 1, AB and CD, and assume that H17A can be included in the AB cross-section (Figure 2a).

[4] A preliminary analysis of this data revealed that only stations H17A and LKWY have particle motions appropriated for receiver function studies because the vertical and radial motions have the same sign for the initial *P*-arrivals, up and away or down and back. Thus, we will use these two stations to perform a detailed study of phases involving *P*-to-*S* conversions. This technique isolates the near-receiver propagation effects [*Zhu et al.*, 1995]. If a low velocity layer is embedded in the upper crust, two *P*-to-*S* phases, which correspond to the *P*-to-*S* converted phases at the top and bottom of the LVZ, will appear after the direct *P* wave on radial-component receiver functions.

2. Seismic Modeling

[5] We obtained and analyzed receiver functions recorded by station H17A and LKWY for 100 common events with details on analysis given in auxiliary material, see Figures S2–S6. The three phases for waves coming from

[1]Seismological Laboratory, California Institute of Technology, Pasadena, California, USA.
[2]Department of Earth and Atmospheric Sciences, Saint Louis University, Saint Louis, Missouri, USA.

0094-8276/10/2009GL041656$05.00

[3]Auxiliary materials are available in the HTML. doi:10.1029/2009GL041656.

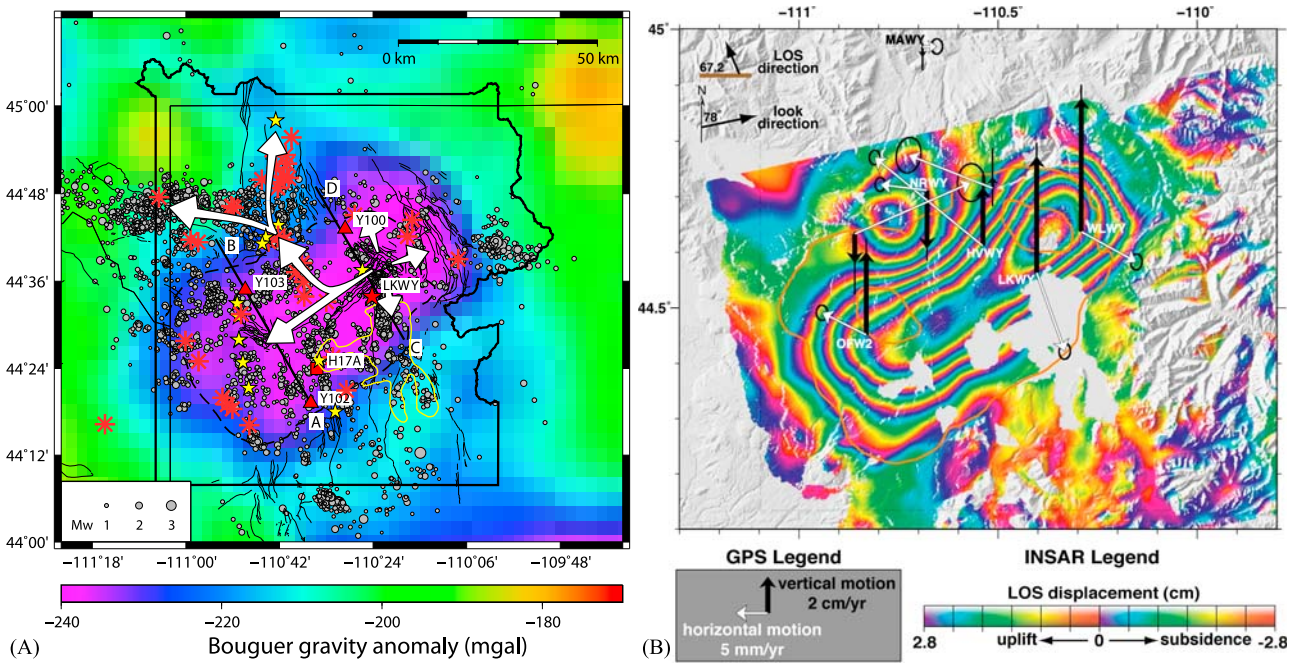

Figure 1. (a) Complete Bouguer gravity anomaly map of the Yellowstone area showing structural, hydrothermal, volcanic, geophysical and seismological features [*Phillips et al.*, 1993]. The solid thick contour marks the boundary of the Yellowstone National Park. The dashed line denotes the boundary of the Yellowstone Caldera generated by the eruption 0.64 Ma ago. Red stars are locations of post-caldera volcanic vents and yellow stars stand for mapped hydrothermal features. The interpreted magma migration paths are shown by arrows [*Wicks et al.*, 2006]. Thin lines are Quaternary faults. Earthquakes with $M_L \geq 1.0$ between 2000 and 2008 are shown by gray circles whose size represents magnitude [*Pechmann et al.*, 2007; *Smith et al.*, 2009]. Broadband seismic stations include H17A (red squares), LKWY (red star), and Y100, Y102, and Y103 (red triangles). The yellow contour indicates the position of Yellowstone Lake. (b) The stacked SAR interferogram and GPS velocities between 2004 and 2006 show uplift of the caldera (reprinted with permission from *Chang et al.* [2007], American Association for the Advancement of Science, http://www.sciencemag.org). See caption of Figure 2 of *Chang et al.* [2007] for details. The rapid changes in ground uplift are compatible with about 0.1 km^3 magma change in volume yearly [*Chang et al.*, 2007]. The shape of the magma body agrees with the purple area suggested by the low gravity anomaly.

southeast of H17A can be easily identified (Figure 2a). The first positive pulse is the direct *P* wave that travels through the LVZ (labeled as 1 in Figure 2a). The negative-amplitude phase 2 and positive-amplitude phase 3 are the *P*-to-*S* converted phases from the top and bottom of the LVZ, respectively (Figure 2b). Phases after 3 sec are multiples trapped above the LVZ (Figure S4). By modeling the radial receiver functions, we obtained a model with two layers over a half space, which appears to be the simplest model found to still explain these waveforms (Figure 2c). The best-fitting velocity model for southeast of station H17A has a horizontal LVZ at a depth of 9.0 km with a thickness of 3.6 km. The *S*-wave velocity drops 66% from 3.30 km/sec to 1.10 km sec with $V_p/V_s = 2.08$ (Figures S5 and S6). Such low values have been obtained from detailed reflection modeling of the magma body beneath Mt. Vesuvius [*Auger et al.*, 2001]. For northwest of H17A, the LVZ is dipping southeast at a depth of 5.5 km with a small dip of a few degrees.

[6] This shallow LVZ beneath the Yellowstone Caldera is severe enough to cause difficulties with seismic tool applications. In particular, seismologists expect teleseismic *P*-waves to arrive with motions up and away or down and back as mentioned earlier. Synthetic teleseismic waveforms, however, violate this assumption in some circumstances when the LVZ is severe enough. For instance, stations near the trailing edge have reversal radial-component motions, while stations near the leading edge do not (Figures S7–S11). Wave propagation simulations show that if the LVZ is slow enough, *P* waves can wrap around the ends to reach the receivers before the direct arrivals.

[7] Many of the observations recorded by the YISA stations display the reversed radial components. For example, teleseismic waves coming from southeast recorded by station Y103 have different polarities on the radial and vertical components, while its radial and vertical motions have the same polarities for waves coming from northwest (Figure 2d). This phenomenon is not produced by the wrong alignment of instruments (supplementary information with Figure S12). Moreover, the radial component of Y102 flips for northwest arriving waves. These two stations confirm the existence of the LVZ beneath the Yellowstone Caldera. If the LVZ has a smaller velocity drop (33% for example), the radial and vertical components will have the same polarities (Figure 2d, lower two rows), which obviously does not fit the observed data. Based on the receiver function

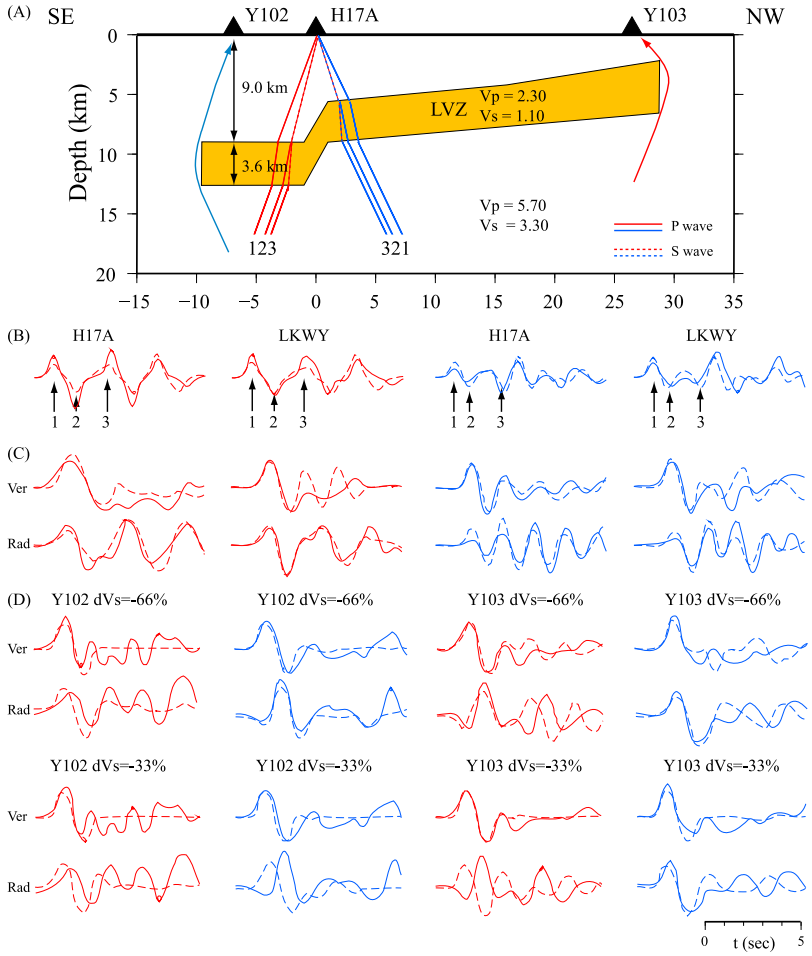

Figure 2. (a) Velocity structures beneath station H17A and LKWY inferred from receiver function modeling. Various ray paths from southeast (red) and northwest (blue) are identified. An ultra low velocity zone (LVZ) is embedded in the upper crust beneath the Yellowstone Caldera with a thickness of 3.6 km with V_p = 2.29 km/sec, V_s = 1.10 km/sec. On the southeast side, the LVZ is a horizontal layer at a depth of 9.0 km. On the northwest, the LVZ is dipping with an angle of 2° at 5.4 km. The ray paths, 1, 2 and 3, are direct *P* wave through the LVZ, *P*-to-*SV* converted phase from top of the LVZ and *P*-to-*SV* phase from bottom of the LVZ, respectively. Solid and dotted lines indicate P and SV waves, respectively. The horizontal dimension of the LVZ agrees with InSAR observations [*Chang et al.*, 2007]. (b) Observed (solid) and synthetic (dashed) receiver functions for stations H17A and LKWY. Different ray paths in Figure 2a are also labeled as they change mode from *P* to *S*. Phases after 3 sec are multiples trapped above the LVZ. (c) Comparison of observed data (solid) and synthetic waveforms (dashed) calculated using finite difference algorithm [*Yan and Clayton*, 2007] and the velocity model from Figure 2a for the vertical and radial component velocity-field. (d) Comparison of waveform data (solid) and synthetics (dashed) for stations Y102 and Y103. If the velocity drop is severe enough (upper two rows, dVs = −66%), the radial component becomes reversed or flipped (Y102 northwest and Y103 southeast) as observed. Otherwise, radial and vertical components have the same polarities (lower two rows).

modeling and wrap-around waves for stations Y102 and Y103, we obtained an image of the profile along AB (Figure 2a and Figures S13 and S14). The magma body also correlates well with the hydrothermal, volcanic, and seismic features with over 900 earthquakes occurring in the Yellowstone Lake area during the 2008–2009 sequence near the station LKWY (Figure 1a).

[8] Along profile CD, station LKWY has a similar upper-crustal velocity structure to H17A. On the southeastern side of LKWY, the horizontal LVZ is 9.0 km deep. On the northwestern side of LKWY, the LVZ dips southeast at a depth of 5.6 km with an angle of about 2° (Figure S15). For station Y100, its radial component flips for teleseismic waves from northwest, which implies that it sits on a trailing edge. Together with regional earthquake hypocenters, we sketched a cross section in Figure S15. Synthetic waveforms show the same reversal pattern as station Y100 (Figures S16 and S17).

[9] Our discovery of wrap-around phases in combination with receiver function analysis produces a distinctly different physical state of this magma body than previous studies [*Husen et al.*, 2004; *Daniel and Boore*, 1982; *Benz and Smith*, 1984; *Stachnik et al.*, 2008]. The V_p/V_s = 2.08 corresponds to a Poisson's ratio of 0.35. This ultra low V_s and high Poisson's ratio indicate the presence of a magma chamber. *Eaton et al.* [1975] modeled the gravity field using 4

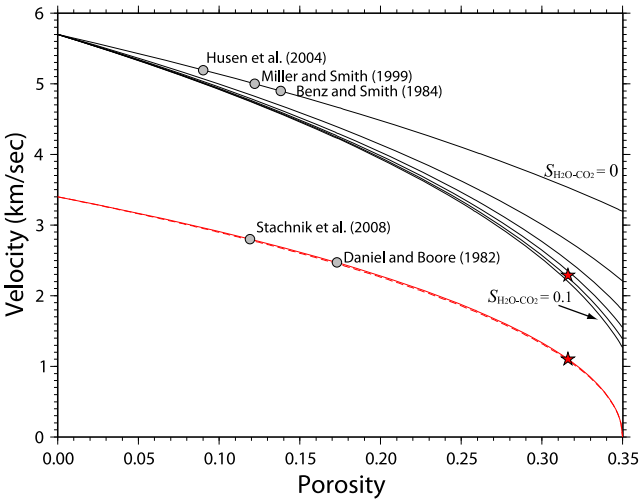

Figure 3. Theoretical compressional (black) and shear (red) velocities in granite as a function of porosity filled with different rhyolite melt and water-CO_2 contents. Red stars denote our modeling velocities suggesting a porosity of 32% and water/CO_2 saturation of 8% by volume. For comparison, we also plotted results from previous studies (gray circles) based on tomography of regional earthquake data [*Benz and Smith*, 1984; *Miller and Smith*, 1999; *Husen et al.*, 2004], inversion of surface wave dispersion [*Daniel and Boore*, 1982], and ambient noise tomography [*Stachnik et al.*, 2008].

different types of source and presented 14 three-dimensional interpretations [*Eaton et al.*, 1975]. Our profiles resemble the cross-sections with molten rhyolite magma. Based on InSAR image modeling that suggests the magma body has an area of about 1,200 km^2 [*Chang et al.*, 2007] (Figure 1b), we estimate the total volume of the magma body of about 4,300 km^3.

3. Results and Conclusions

[10] Using the method described in the auxiliary material, we can estimate the magma body by assuming a fluid-saturated porous granite with various porosity filled with different melt and fluid contents. Because water and CO_2 have almost identical effects on seismic velocities (Figure S18), we combined water-CO_2 saturations in the computation. Figure 3 shows various V_p curves corresponding to different fluid saturations from 0% to 10% with an increment of 2%. The corresponding V_s curves are not distinguishable. It is clear that adding water/CO_2 to the magma will not change the shear velocity much. The compressional velocity, however, changes significantly, especially when the porosity approaches the critical porosity. The P and S velocities obtained from our modeling suggest that the magma body has a porosity of about 32% filled with at least 90% rhyolite melt and 8% water-CO_2 by volume (Figure 3). In situ measurements of water/CO_2 ratio for volcanic gasses is 2.2 by weight [*Chiodini et al.*, 2001]. If we assume that 50% of the daily emission of CO_2 is degassed from the magma body [*Werner and Brantley*, 2003], CO_2 in the magma body will be released completely in about 1,100 years, which is much less than 15,000 years suggested by *Fournier* [1989]. Perhaps a basaltic magma chamber exists in the uppermost mantle supplying this large budget of CO_2 [*Lowenstern and Hurwitz*, 2008].

[11] **Acknowledgments.** We are grateful to two GRL reviewers for their careful reviews. We thank Robert W. Clayton for the constructive discussions. The 2D finite difference modeling code was provided by Zhimei Yan. All waveform data used in this study were obtained from IRIS Data Management Center. This work is funded by the Tectonics Observatory at California Institute of Technology under grant GPS.TO2-4.1-GRANT. MOORETO2. This is contribution 10035 of the Tectonics Observatory at Caltech.

References

Auger, E., P. Gasparini, J. Virieux, and A. Zollo (2001), Seismic evidence of an extended magmatic sill under Mt. Vesuvius, *Science*, *294*, 1510–1512, doi:10.1126/science.1064893.

Benz, H. M., and R. B. Smith (1984), Simultaneous inversion for lateral velocity variations and hypocenters in the Yellowstone region using earthquake and refraction data, *J. Geophys. Res.*, *89*, 1208–1220.

Chang, W. L., R. B. Smith, C. Wicks, J. M. Farrell, and C. M. Puskas (2007), Accelerated uplift and magmatic intrusion of the Yellowstone Caldera, 2004 to 2006, *Science*, *318*, 952–956.

Chiodini, G., F. Frondini, C. Cardellini, D. Granieri, L. Marini, and G. Ventura (2001), CO_2 degassing and energy release at Solfatara Volcano, Campi Flegrei, Italy, *J. Geophys. Res.*, *106*, 16,213–16,221.

Christiansen, R. L. (2001), The Quaternary and Pliocene Yellowstone plateau volcanic field of Wyoming, Idaho, and Montana, *U.S. Geol. Surv. Prof. Pap.*, *729-G*.

Daniel, R. G., and D. M. Boore (1982), Anomalous shear wave delays and surface wave velocities at Yellowstone Caldera, Wyoming, *J. Geophys. Res.*, *87*, 2731–2744.

Eaton, G. P., R. L. Christiansen, H. M. Iyer, A. D. Pitt, D. R. Mabey, H. R. Blank Jr., I. Zietz, and M. E. Gettings (1975), Magma beneath Yellowstone National Park, *Science*, *188*, 787–796.

Fournier, R. O. (1989), Geochemistry and dynamics of the Yellowstone National Park hydrothermal system, *Annu. Rev. Earth Planet. Sci.*, *17*, 13–53.

Husen, S., R. B. Smith, and G. P. Waite (2004), Evidence for gas and magmatic sources beneath the Yellowstone volcanic field from seismic tomographic imaging, *J. Volcanol. Geotherm. Res.*, *131*, 397–410.

Lowenstern, J. B., and S. Hurwitz (2008), Monitoring a supervolcano in repose: Heat and volatile flux at the Yellowstone Caldera, *Elements*, *4*, 35–40.

Lowenstern, J. B., R. B. Smith, and D. P. Hill (2006), Monitoring supervolcanoes: Geophysical and geochemical signals at Yellowstone and other large caldera systems, *Philos. Trans. R. Soc. Ser. A*, *364*, 2055–2072.

Miller, D. S., and R. B. Smith (1999), *P* and *S* velocity structure of the Yellowstone volcanic field from local earthquake and controlled-source tomography, *J. Geophys. Res.*, *104*, 15,105–15,121.

Pechmann, J. C., S. J. Nava, F. M. Terra, and J. C. Bernier (2007), Local magnitude determinations for intermountain seismic belt earthquakes from broadband digital data, *Bull. Seismol. Soc. Am.*, *97*, 557–574, doi:10.1785/0120060114.

Phillips, J. D., J. S. Duval, and R. A. Ambroziak (1993), National geophysical data grids: Gamma-ray, gravity, magnetic and topographic data for the conterminous United States, *U.S. Geol. Surv. Digital Data Ser.*, *DDS-9*.

Puskas, C. M., R. B. Smith, C. M. Meertens, and W. L. Chang (2007), Crustal deformation of the Yellowstone–Snake River Plain volcano-tectonic system: Campaign and continuous GPS observations, 1987–2004, *J. Geophys. Res.*, *112*, B03401, doi:10.1029/2006JB004325.

Smith, R. B., M. Jordan, B. Steinberger, C. M. Puskas, J. Farrell, G. P. Waite, S. Husen, W.-L. Chang, and R. O'Connell (2009), Geodynamics of the Yellowstone hotspot and mantle plume: Seismic and GPS imaging, kinematics, and mantle flow, *J. Volcanol. Geotherm. Res.*, *188*, 26–56, doi:10.1016/j.jvolgeores.2009.08.020.

Stachnik, J. C., K. Dueker, D. L. Schutt, and H. Yuan (2008), Imaging Yellowstone plume-lithosphere interactions from inversion of ballistic and diffusive Rayleigh wave dispersion and crustal thickness data, *Geochem. Geophys. Geosyst.*, *9*, Q06004, doi:10.1029/2008GC001992.

Waite, G. P., and R. B. Smith (2002), Seismic evidence for fluid migration accompanying subsidence of the Yellowstone Caldera, *J. Geophys. Res.*, *107*(B9), 2177, doi:10.1029/2001JB000586.

Werner, C., and S. Brantley (2003), CO_2 emissions from the Yellowstone volcanic system, *Geochem. Geophys. Geosyst.*, *4*(7), 1061, doi:10.1029/2002GC000473.

Wicks, C. W., W. Thatcher, and D. Dzurisin (1998), Migration of fluids beneath Yellowstone Caldera inferred from satellite radar interferometry, *Science*, *282*, 458–462.

Wicks, C. W., W. Thatcher, D. Dzurisin, and J. Svarc (2006), Uplift, thermal unrest and magma intrusion at Yellowstone Caldera, *Nature*, *440*, 72–75.

Yan, Z., and R. W. Clayton (2007), A notch structure on the Moho beneath the eastern San Gabriel Mountains, *Earth Planet. Sci. Lett.*, *260*, 570–581.

Zhu, L., T. J. Owens, and G. E. Randall (1995), Lateral variation in crustal structure of the northern Tibetan Plateau inferred from teleseismic receiver function, *Bull. Seismol. Soc. Am.*, *85*, 1531–1540.

R. Chu, D. V. Helmberger, J. M. Jackson, and D. Sun, Seismological Laboratory, California Institute of Technology, Pasadena, CA 91125, USA. (chur@gps.caltech.edu)

L. Zhu, Department of Earth and Atmospheric Sciences, Saint Louis University, St. Louis, MO 63108, USA. (lupei@eas.slu.edu)